

**PS Evaluation of Potential Geochemical Reactions and Changes in Hydrologic Properties  
at the Kemper County CO<sub>2</sub> Storage Complex\***

**Lauren E. Beckingham<sup>1</sup>, Fanqi Qin<sup>1</sup>, Ishan Anjekar<sup>1</sup>, Brenda L. Kirkland<sup>2</sup>, and Shawna Cyphers<sup>3</sup>**

Search and Discovery Article #80653 (2018)\*\*

Posted November 19, 2018

\*Adapted from poster presentation given at 2018 AAPG Annual Convention & Exhibition, Salt Lake City, Utah, May 20-23, 2018

\*\*Datapages © 2018 Serial rights given by author. For all other rights contact author directly. DOI:10.1306/80653Beckingham2018

<sup>1</sup>Civil Engineering, Auburn University, Auburn, Alabama ([leb@auburn.edu](mailto:leb@auburn.edu))

<sup>2</sup>Mississippi State University, Starkville, Mississippi

<sup>3</sup>Advanced Resources International, Knoxville, Tennessee

**Abstract**

Following CO<sub>2</sub> injection, CO<sub>2</sub>-brine-mineral interactions may result in mineral dissolution and precipitation reactions that impact rock properties including porosity, permeability, and pore connectivity. The extent and timescale of these alterations largely depend on the reservoir rock properties including the nature and distribution of reactive mineral interfaces. In this work, the potential rate and extent of geochemical reactions and changes in hydrologic properties at the CO<sub>2</sub> Storage Complex in Kemper County, Mississippi, USA (Project ECO<sub>2</sub>S) is evaluated. At this site, the Lower Tuscaloosa, Washita-Fredericksburg, and Paluxy formations have been identified as future regionally extensive and attractive CO<sub>2</sub> storage reservoirs. Here, a suite of complementary analyses including powder X-ray Diffraction (XRD) and 2D scanning electron microscopy (SEM) backscattered electron (BSE) and energy dispersive x-ray spectroscopy (EDS) imaging is used in combination with reactive transport simulations to evaluate potential geochemical reactions and changes in formation properties following CO<sub>2</sub> injection.

Formation samples obtained from potential injection and monitoring wells at the site are evaluated and compared with analyses of regional samples of the formations obtained from the Geological Survey of Alabama. Mineral compositions, determined using petrography and XRD, are used to develop continuum-scale reactive transport simulations to identify potential CO<sub>2</sub>-brine-mineral interactions with a focus on identifying potential reactive minerals and the corresponding rate and extent of reactions. Mineral reaction rates and changes in the pore structure, including pore connectivity, porosity, and permeability, depend on the spatial distribution and accessibility of minerals to reactive fluids. Spatial maps of mineral distribution will be created using 2D SEM imaging and used to evaluate the nature of the pore-mineral interface, the distribution and accessibility of reactive minerals, and the potential for flow-path modifications resulting from mineral dissolution reactions following CO<sub>2</sub> injection.

The “Establishing an Early CO<sub>2</sub> Storage Complex in Kemper, MS” project is funded by the U.S. Department of Energy’s National Energy Technology Laboratory and cost-sharing partners.

## Abstract

Following CO<sub>2</sub> injection, CO<sub>2</sub>-brine-mineral interactions may result in mineral dissolution and precipitation reactions that impact rock properties including porosity, permeability, and pore connectivity. The extent and timescale of these alterations largely depend on the reservoir rock properties including the nature and distribution of reactive mineral interfaces. In this work, the potential rate and extent of geochemical reactions and changes in hydrologic properties at the CO<sub>2</sub> Storage Complex in Kemper County, Mississippi, USA (Project ECO2 S) is evaluated. At this site, the Lower Tuscaloosa, Washita-Fredericksburg, and Paluxy formations have been identified as future regionally extensive and attractive CO<sub>2</sub> storage reservoirs. Here, a suite of complementary analyses including powder X-ray Diffraction (XRD) and 2D scanning electron microscopy (SEM) backscattered electron (BSE) and energy dispersive x-ray spectroscopy (EDS) imaging is used in combination with reactive transport simulations to evaluate potential geochemical reactions and changes in formation properties following CO<sub>2</sub> injection. Formation samples obtained from potential injection and monitoring wells at the site are evaluated and compared with analyses of regional samples of the formations obtained from the Geological Survey of Alabama. Mineral compositions, determined using petrography and XRD, are used to develop continuum-scale reactive transport simulations to identify potential CO<sub>2</sub>-brine-mineral interactions with a focus on identifying potential reactive minerals and the corresponding rate and extent of reactions. Mineral reaction rates and changes in the pore structure, including pore connectivity, porosity, and permeability, depend on the spatial distribution and accessibility of minerals to reactive fluids. Spatial maps of mineral distribution will be created using 2D SEM imaging and used to evaluate the nature of the pore-mineral interface, the distribution and accessibility of reactive minerals, and the potential for flow-path modifications resulting from mineral dissolution reactions following CO<sub>2</sub> injection. The "Establishing an Early CO<sub>2</sub> Storage Complex in Kemper, MS" project is funded by the U.S. Department of Energy's National Energy Technology Laboratory and cost-sharing partners

## Reactive transport modeling

### Mineralization of CO<sub>2</sub>

CO<sub>2</sub> dissolution in brine:  $\text{CO}_2 + \text{H}_2\text{O} = \text{H}^+ + \text{HCO}_3^-$   
 Primary mineral dissolution<sup>[4]</sup>:  $2\text{H}^+ + \text{CaAl}_2\text{Si}_2\text{O}_8 + \text{H}_2\text{O} = \text{Ca}^{2+} + \text{Al}_2\text{Si}_2\text{O}_7(\text{OH})_4$   
 Calcite precipitation:  $\text{Ca}^{2+} + \text{HCO}_3^- = \text{CaCO}_3 + \text{H}^+$

### Reactive transport model



Simulations of CO<sub>2</sub>-brine-mineral reactions were carried out using CrunchFlow. In this system, Supercritical CO<sub>2</sub> is in equilibrium with brine in the first cell, then flows into mineral cell where mineral volume fractions and accessibility are gained from imaging analyses.

### Dissolution rate

$$R_{\text{mineral}} = A_r k \left(1 - \frac{Q}{K}\right)^\alpha \quad (\text{Transition State Theory})$$

where  $A_r$  is the reactive surface area,  $k$  is the absolute kinetic rate constant,  $Q$  is the ion activity product of the mineral in solution,  $K$  is the equilibrium ion activity product of the mineral in solution,  $\alpha$  is an empirical constant<sup>[50]</sup>.

### CO<sub>2</sub> properties in three potential storage formations

Table 1. Calculated CO<sub>2</sub> properties in three potential storage formations<sup>[4-5]</sup>.

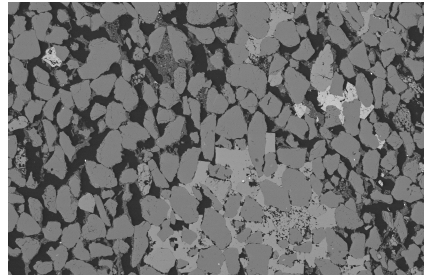
Formation	Temperature (°C)	Pressure (bar)	CO <sub>2</sub> density (kg/m <sup>3</sup> )	CO <sub>2</sub> solubility (mol/kg)
Lower Tuscaloosa	32.86	97.01	743.02	1.05
Washita Fredericksburg	38.58	121.02	746.10	1.03
Paluxy	46.20	153.02	748.10	1.02

### Acknowledgement:

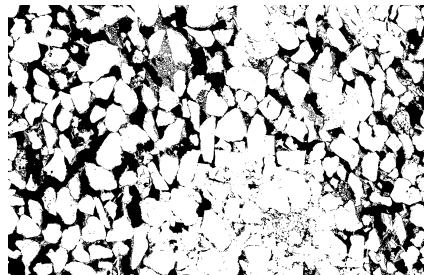
The "Establishing an Early CO<sub>2</sub> Storage Complex in Kemper, MS" project is funded by the U.S. Department of Energy's National Energy Technology Laboratory and cost-sharing partners.

## Imaging Characterization

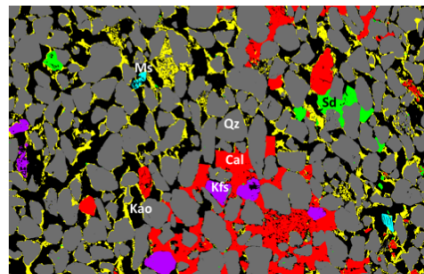
### 2D SEM imaging



Scanning Electron Microscope (SEM) Backscattered Electron (BSE) image of sample from Paluxy formation with resolution of 1.13 μm.

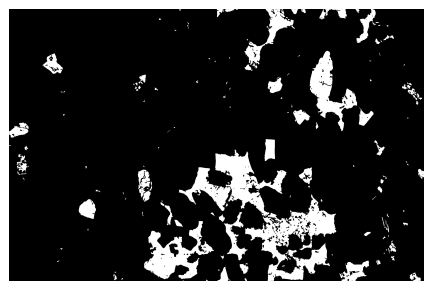


Segmented BSE image depicting pores (black) and grains (white). Porosity = 0.2732.



Segmented mineral map showing: Qz = Quartz; Kao = Kaolinite; Kfs = K-feldspar, Cal = Calcite; Ms = Muscovite, Sd = Siderite.

**Clay minerals (e.g. Kaolinite) have a larger accessible surface area because they are present as grain coatings. The accessible percentage of kaolinite is 51.07% versus volume abundance of 10.14%.**



Potential reactive mineral map. The fraction of reactive mineral phases in this area is 0.1923.

**19.23% of the minerals are reactive. Assuming all of them dissolve, the porosity will increase from 0.27 to 0.36, changing the pore structure and increasing permeability from ~2.3x10<sup>-12</sup> m<sup>2</sup> to ~5.1x10<sup>-12</sup> m<sup>2</sup>.**

### Reference

- Alkattan, M., Oelkers, E.H., Dandurand, J.L. and Schott, J., 1998. *Chem Geol*, 151(1-4), pp.199-214.
- Bevan, J. and Savage, D., 1989. *Mineral Mag*, 53(372), pp.415-425.
- Brady, P.V. and Walther, J.V., 1990. *Chem Geol*, 82, pp.253-264.

## Formation Data

### Mineral abundance and accessibility

Table 2. Mineral distribution from SEM analyses and mineral reaction rates at 33 °C.

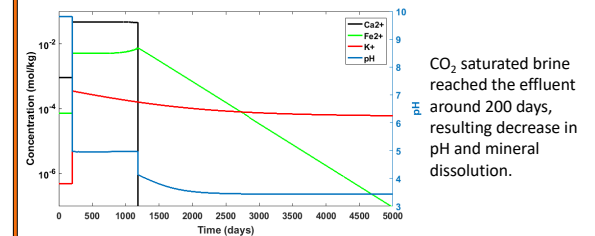
Mineral	Volume percentage (%)	Accessible percentage (%)	Log K (mol·m <sup>-2</sup> ·s <sup>-1</sup> )
Quartz <sup>[3]</sup>	74.57	34.92	-12.03
K-feldspar <sup>[2]</sup>	2.01	1.65	-11.66
Kaolinite <sup>[7]</sup>	10.14	51.07	-12.50
Calcite <sup>[1]</sup>	11.47	10.01	-3.901
Muscovite <sup>[9]</sup>	0.24	1.00	-12.194
Siderite <sup>[8]</sup>	1.57	1.34	-9.97

### Formation brine chemistry

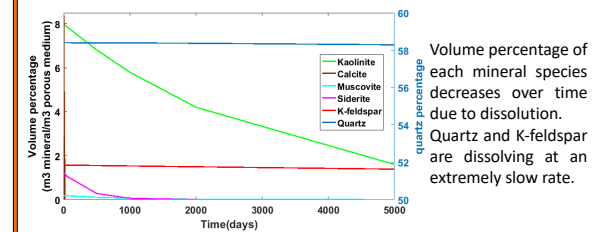
Table 3. Simulated brine chemistry of Paluxy formation.

Major ion	Ca <sup>2+</sup>	Al <sup>3+</sup>	Fe <sup>2+</sup>	K <sup>+</sup>	SiO <sub>2</sub> (aq)	HCO <sub>3</sub> <sup>-</sup>
Concentration (mol/kg)	7.80E-04	1.67E-06	5.83E-05	4.76E-06	9.18E-04	8.39E-04

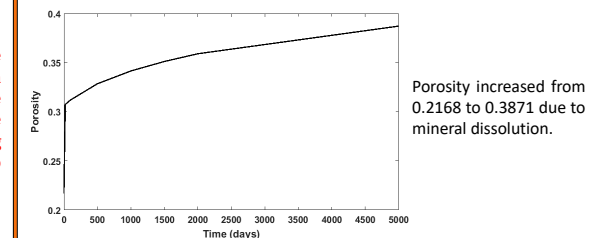
## Simulation Results



CO<sub>2</sub> saturated brine reached the effluent around 200 days, resulting decrease in pH and mineral dissolution.



Volume percentage of each mineral species decreases over time due to dissolution. Quartz and K-feldspar are dissolving at an extremely slow rate.



Porosity increased from 0.2168 to 0.3871 due to mineral dissolution.

- DePaolo, D.J. and Cole, D.R., 2013. *Rev Mineral Geochem*, 77(1), pp.1-14.
- Duan, Z., Moller, N. and Weare, J.H., 1992. *Geochim Cosmochim Acta*, 56(7), pp.2605-2617.
- Duan, Z. and Sun, R., 2003. *Chem Geol*, 193(3-4), pp.257-27
- Ganoc, J., Mogollon, J.L. and Lasaga, A.C., 1995. *Geochim Cosmochim Acta*, 59(6), pp.1037-1052.

- Golubev, S.V., Bénédeth, P., Schott, J., Dandurand, J.L. and Castillo, A., 2009. *Chem Geol*, 265, pp.13-19.
- Kalinowski, B.E. and Schweda, R., 1996. *Geochim Cosmochim Acta*, 60(3), pp.367-385.
- Zhang, S. and DePaolo, D.J., 2017. *Accounts Chem Res*, 50(9), pp.2075-2084.